NEW ZEALAND SOCIETY FOR EARTHQUAKE ENGINEERING

Enhancing Structural Resilience: Three-Dimensional Seismic Isolation (3DSI) in Practice

M. Pourmasoud, A. Park
Robinson Seismic ltd, Hamilton, New Zealand.

I. Hajirashouliha
The university of Sheffield, Sheffield, UK.

J. Lim
The University of Waikato, Hamilton, New Zealand.

ABSTRACT

This research introduces a novel Three-Dimensional Seismic Isolation (3DSI) designed to evaluate the coupled horizontal-vertical responses of a five-story building. A comprehensive structural analysis using the OpenSees software was conducted for three distinct structural systems: the traditional Fixed Base (F.B.) system, the Conventional Seismic Isolated (CSI) structure, and the Three-Dimensional Seismic Isolated (3DSI) building. The proposed 3DSI system is based on the utilization of Super-High-Damping-Rubber (SHDR) technology, which is engineered to achieve vertical isolation. This is achieved through the reduction of vertical effective stiffness and the simultaneous increase in vertical effective damping, resulting in the minimization of vertical acceleration imparted to the superstructure. The research findings demonstrate that the 3DSI system substantially decreases both vertical and horizontal responses by up to 65% and 20% respectively when compared to the CSI system. In contrast, both the F.B. and CSI buildings exhibit amplification in vertical accelerations, particularly in the case of long-span beams, leading to extensive non-structural damage. Moreover, the 3DSI system results in reduced compression and tension axial loads, along with diminished story drifts.

1 INTRODUCTION

The performance of structural elements depends significantly on story drift, while non-structural elements are more sensitive to acceleration. For essential buildings such as hospitals, over 90% of the project cost is allocated to non-structural elements and contents (FEMA E-74 2012). The coupling of horizontal-vertical excitations might cause medium to complete damage to non-structural elements (Pourmasoud et al. 2020 and

Cancellara and De Angelis 2016). Although Conventional Seismic Isolators (CSI) are effective in reducing floor accelerations, they are not suitable for mitigating vertical responses in structures (Dong et al. 2023 and Guzman Pujols and Ryan 2018). In a building, the objects start to shake when vertical acceleration exceeds 1.0g and damage happens when it goes beyond 2.0g (Furukawa et al. 2013). Experimental test results show that vertical accelerations between 2.0 and 5.0g can cause moderate to extensive damage, and buildings with higher vertical accelerations may suffer complete non-structural damage (Ryan et al. 2016 and Soroushian et al. 2016).

In recent years, there has been a growing interest in the development of three-dimensional seismic isolators, as building in near field zones with high vertical peak ground acceleration (PGA) is unavoidable in many regions. For example, Wellington (New Zealand), California (USA), and Jakarta (Indonesia) are among the cities where buildings and infrastructure have extended in the vicinity of active faults. Therefore, the new generation of seismic isolation systems shall replace Conventional Seismic Isolators (CSIs) with Three Dimensional Seismic Isolators (3DSIs) to effectively mitigate both horizontal and vertical ground motions.

A new concept for a 3D seismic isolation system (3DSI) was proposed in 2020 with the objective of developing a system that could increase the vertical effective damping and decrease the vertical responses, while maintaining all the horizontal specifications of an elastomer bearing (Pourmasoud et al. 2020). To achieve this, a Super High Damping Rubber (SHDR) layer, which is horizontally curved against lateral movements, was added to a Lead Rubber Bearing (LRB) to provide vertical stiffness and damping. This enabled the vertical specifications to be adjustable without impacting the horizontal specifications. Figure. 1 depicts the proposed 3DSI before and after lateral displacement. The total vertical stiffness of the proposed 3DSI comprises the vertical stiffness of the LRB at a certain lateral displacement, as well as the vertical stiffness of the SHDR layers.

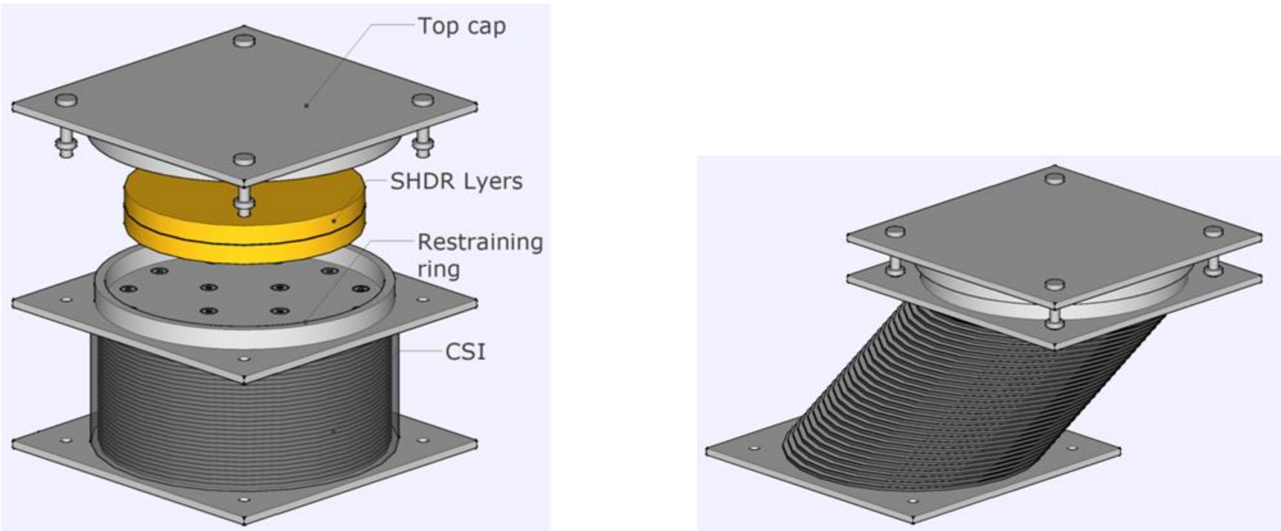

Figure. 1. 3DSI with SHDR layers.

2 NUMERICAL STUDY

2.1 Super structure

A case study of a multi-story building was implemented using the OpenSees software. The structure was modelled as a dual system consisting of intermediate steel moment frames and braces. The floor height is 4m, and it is divided into three spans of 6.0m and 9.0m to investigate the influence of vertical acceleration on medium and long spans. The structural elements were designed based on the requirements of a high seismic zone, as specified in the ASCE 7-22 (2022). Figure. 2 shows the 2D fixed base model developed in OpenSees.

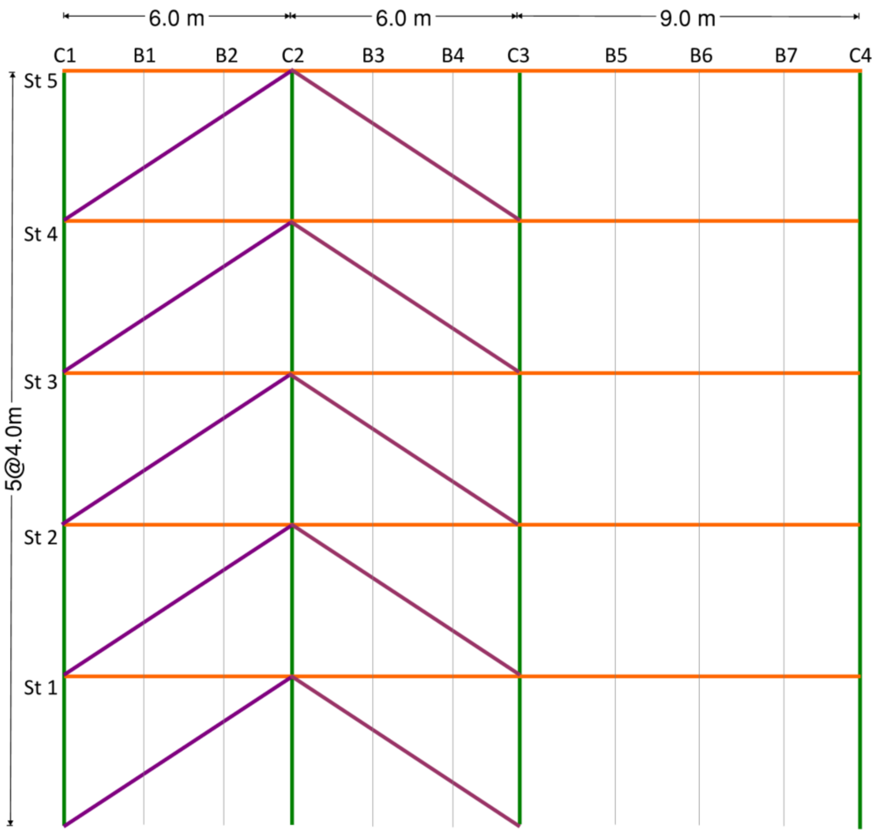

Figure. 2. 2D OpenSees model.

2.2 Seismic Isolation Systems

In order to investigate the influence of the proposed 3DSI on the performance of super-structure, three seismic system were implemented, including:

1. Fixed Base (FB).

2. Conventional Seismic Isolation (CSI) system, which is a lead rubber bearing to provide the horizontal isolation.

3. 3DSI, which is a combination of lead rubber bearing and SHDR layers to mitigate the horizontal-vertical responses.

Figure. 3 shows the DBE and MCE response spectrums which are from a high seismic region in Wellington, New Zealand and used to design the LRB isolator which comprises of 26@10mm rubber layers and a 170mm diameter lead core.

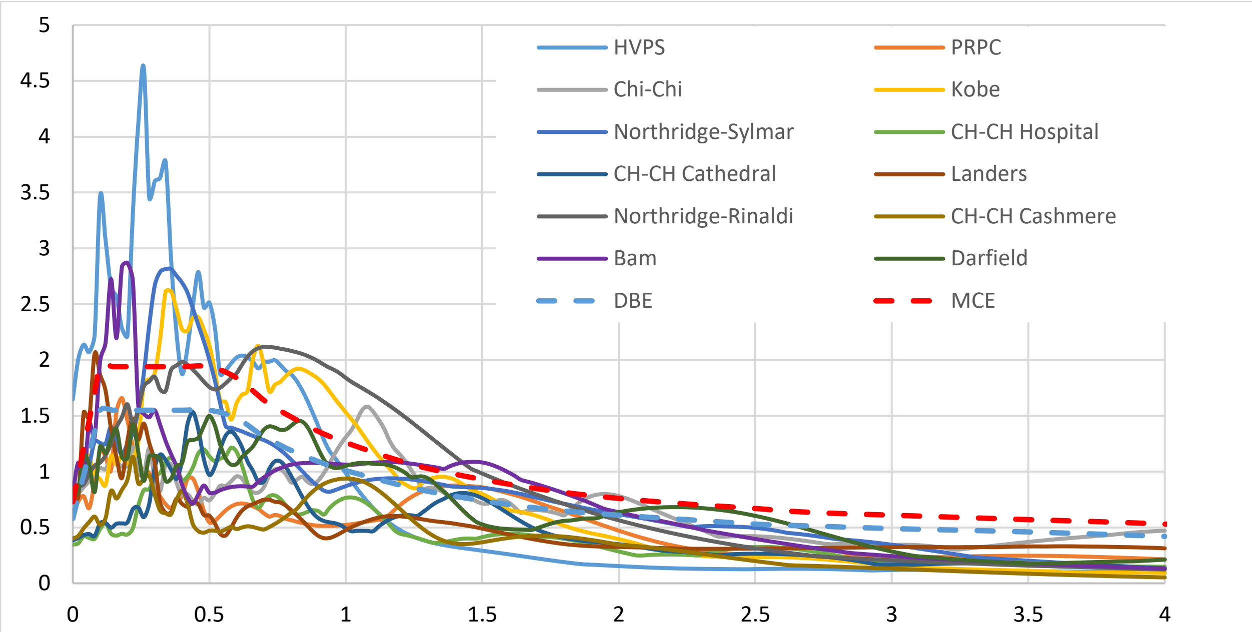

Figure. 3. The horizontal acceleration spectrums.

The LRB was tested under a variety of lateral displacements and compression loads to measure the mechanical specifications at each step. Figure. 4 and Table 1 demonstrate the LRB's hysteresis loops and the corresponding mechanical specifications.

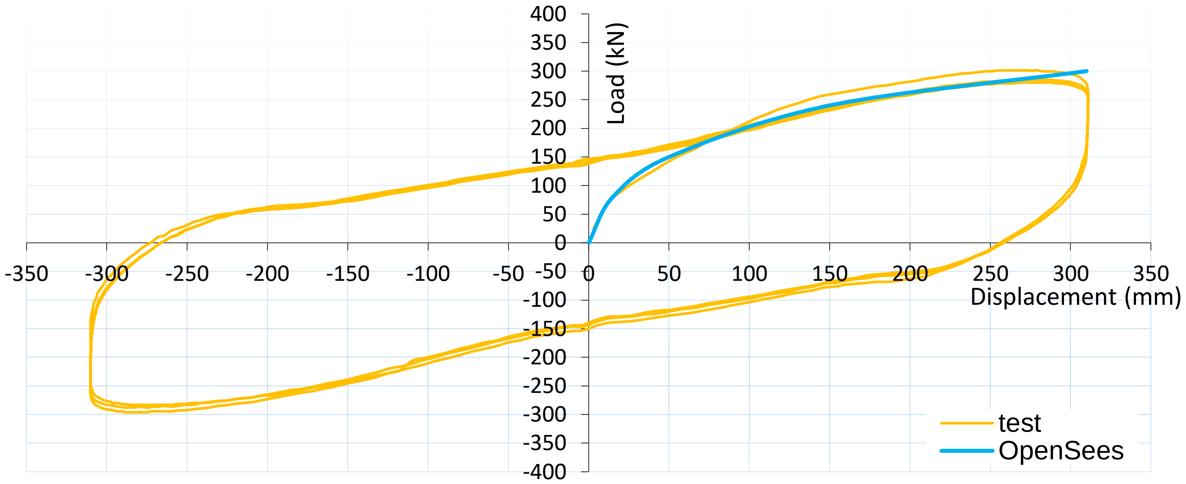

Figure. 4. The LRB hysteresis loop.

Table 1. the LRB test results.

Cycle	*Disp Min (mm)*	*Disp Max (mm)*	*Load Min (kN)*	*Load Max (kN)*	*Area (kNm)*	*k effective (kN/mm)*	*Damping %*
1	*-310.1*	*311.1*	*-296.0*	*301.6*	*185.1*	*0.962*	*31.7*
2	*-310.1*	*311.1*	*-287.9*	*286.2*	*180.6*	*0.924*	*32.2*
3	*-310.1*	*311.1*	*-284.7*	*280.0*	*176.9*	*0.909*	*32.1*

To model the horizontal behaviour of an isolator in OpenSees, the Multilinear Material link is an ideal option. The software can be allocated with the deformation and force (or strain and stress) at each step of the envelope to shape a cycle of loading. In this case, three spots were introduced to the software to shape the LRB hysteresis loop.

3 EXPERIMENTAL TESTS

In order to determine a practical range of vertical stiffness, nine SHDR layers were created and tested under cyclic loads. These layers represent a high level of damping compared to normal rubber layers and were all 600mm in diameter. Various thicknesses of 30, 40, and 50mm, as well as different shear moduli of G60, G80, and G100, were considered. Under 2500 kN cyclic loads, the rubber layers were compressed to investigate their vertical stiffness, bulging, shear strain due to compression, and potential vertical effective damping. Table 1 presents the dimension and mechanical specification of the SHDR layers under the applied axial load.

Table 1. Rubber layers' vertical stiffness and compression strain.

	Vertical stiffness (kN/mm)			*Shear strain due to compression, $\varepsilon_{C,E}$*		
Thickness (mm) / *G modulus (MPa)*	***50***	***40***	***30***	***50***	***40***	***30***
G 60	*174*	*331*	*769*	*5.2*	*4.2*	*3.2*
G 80	*227*	*430*	*997*	*4.0*	*3.3*	*2.5*
G 100	*276*	*522*	*1207*	*3.3*	*2.7*	*2.1*

The total vertical stiffness of a lead rubber bearing (LRB) at zero displacement is based on the philosophy of series springs, which is equal to the stiffness of a single layer divided by the number of rubber layers. This stiffness will decrease with increasing lateral displacement and can be calculated using Equation (1), (2) as presented by Constantinou et al. (2007).

$$K_{V\,(CSI)} = K_{V0}\left[1 + \frac{3}{\pi^2}\left(\frac{u_h}{r}\right)^2\right]^{-1} \quad (1)$$

$$K_{V0} = \frac{AE_c}{T_r} \quad (2)$$

where uh is the lateral displacement, r is the radius of gyration of the bonded rubber area, A is the bonded area of rubber layer, Ec is the compression modulus and Tr is the total thickness of rubber. For the 3DSI device, the vertical stiffness of SHDR layers will be combined with the stiffness gains from Equation (1) to achieve a low enough stiffness while maintaining the axial loading capacity. Table 3 represents the vertical specifications of SHDR 600x50 – G60. The vertical period (T_v), compression strain (ε_c) and shear strain due to compression load (ε_{sc}), energy dissipation per cycle (EDC) and effective damping (β) are reported. To approach an ideal 3DSI, three layers of SHDR were piled up and the device's total vertical stiffness was calculated. Table 4 presents the CSI vertical stiffness at zero and maximum displacement. So, the dominant vertical period will be 0.41s and 0.34s for the softest and stiffest layers, respectively. In order to define the effective stiffness of the 3DSI to OpenSees, the average stiffness from the first three cycles of SHDR 600x50 combined with the CSI vertical stiffness at the designed maximum displacement was employed.

Table 3. SHDR 600x50 – G60 test results.

SHDR (1 layer)

Cycle		Deformation (mm)	Bulging (mm)	K_v (kN/mm)	Tv	ε_c	ε_{sc}	EDC	β
1	0	0.00	0.00	228.05	0.21	0.22	3.9	10728.125	24.9%
	2500	10.96	71.18						
2	0	8.58	63.81	651.47	0.12	0.08	1.4	1784.375	11.8%
	2500	12.42	91.63						
3	0	10.01	84.90	728.86	0.12	0.07	1.2	1521.875	11.3%
	2500	13.44	97.91						
			Ave.	**536.13**	**0.14**				

Table 2. CSI vertical stiffness at zero and maximum displacement.

E_c (MPa)	A (mm^2)	Tr (mm)	u (mm)	r	K_{v0} (kN/mm)	K_v (kN/mm)
658	418539	260	310	182.50	1059.26	282.07

Figure. 2 illustrates the vertical stiffness diagram of the designed 3DSI to be defined in OpenSees software based on the combination of a conventional isolator and layers of SHDRs.

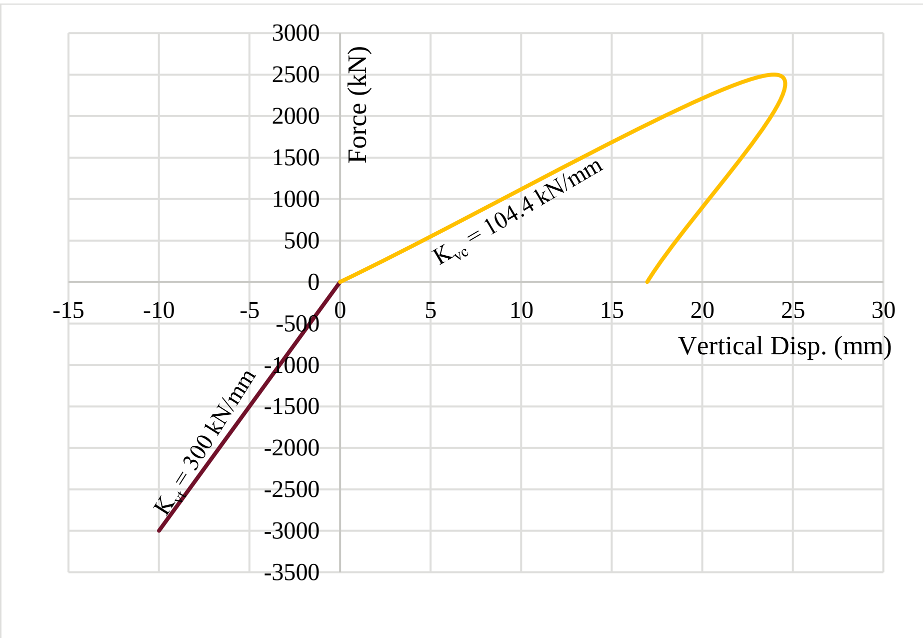

Figure. 2. 3DSI Vertical stiffness.

4 EARTHQUAKE EXCITATIONS

To investigate the 3DSI influence on the performance of the structure, 10 nearfield earthquakes, mostly with high vertical peak ground acceleration (PGA), were selected from the Pacific Earthquake Engineering Research Centre (PEER), as listed in Table 5.

Table 5. Selected ground motions and the PGAs in horizontal and vertical directions

No.	Records	Station	Vertical PGA (g)	Horizontal PGA (g)	Pulse period (s)	M_W	V_{PGA}/H_{PGA}
Eq.1	Chichi	TCU 065	0.27	0.82	5.7	7.6	0.33
Eq.2	Kobe	JMA	0.34	0.83	7.8	6.9	0.41
Eq.3	Northridge	Sylmar	0.53	0.84	3.1	6.7	0.63
Eq.4	Christchurch	Hospital	0.6	0.35	7	6.2	1.71
Eq.5	Christchurch	Cathedral	0.8	0.38	5.6	6.2	2.11
Eq.6	Landers	Lucerne	0.82	0.79	5.1	7.3	1.04
Eq.7	Christchurch	Cashmere	0.85	0.4	6.3	6.2	2.43
Eq.8	Northridge	Rinaldi	0.96	0.87	3	6.7	1.10
Eq.9	Bam	Bam	0.97	0.8	19	6.6	1.21
Eq.10	Darfield	GDLC	1.25	0.71	19.8	7.0	1.76
Eq.11	Christchurch	PRPS*	1.9	0.6	3.34	6.2	3.17
Eq.12	Christchurch	HVPS**	2.18	1.65	2.65	6.2	1.32

*Pages Road Pumping Station

**Heathcote Valley Primary School

Figure. 3 demonstrates the vertical elastic response spectrum for the chosen seismic restricted to 0.8s. This figure illustrates that the vertical periods around 0.1s, which represent the vertical period of most conventional isolators, magnify the vertical acceleration. Vertical accelerations less than 1.0g are not harmful to non-structural elements; accelerations between 1.0 to 2.0g cause shaking of objects and once the vertical acceleration goes beyond 2.0g, tossing and falling of the objects will be expected. So, increasing the vertical period up to 0.3s significantly decreases the acceleration below 2.0g regardless of the vertical damping influence.

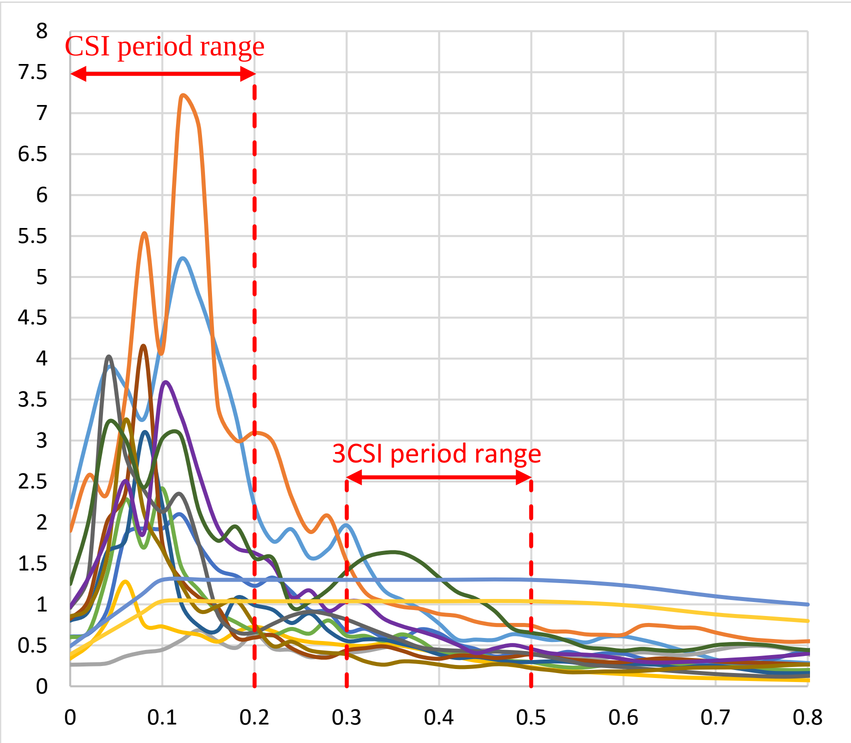

Figure. 3. Vertical response spectrum for 12 selected ground excitations.

5 DISCUSSION AND RESULTS

The aim of this section is to investigate the influence of the 3DSI on the building's responses and compare them with the CSI and FB options. Table 6 presents the vertical accelerations (VA) at the spots of columns and the beams as illustrated in Figure. 2. For each structural system, the accelerations at each column, two spots on the 6m beams, and three spots on the 9m beams were considered. In Table 6, accelerations less than 2.0g are highlighted in green, accelerations up to 4.0g and 5.0g are shown in yellow and orange, respectively, and any acceleration exceeding 5.0g is presented in light red. As it was expected, the fixed base option caused vertical accelerations to gradually increase from bottom to top of columns as well as from end of the beams toward the centre of beams. The CSI option led to amplification of vertical PGA due to low vertical flexibility of isolators which magnify the accelerations from bottom of the device to top of it. In this case, the VAs on the columns is almost as twice as the VAs attained from the fixed base option. Three dimensional isolation has degraded the vertical accelerations up to 65% compare to the CSI option. In this case, the VA decreased from 3.9g to 1.6g on top of the C1 isolation and from 9.3g to 3.3g in the middle of the long beam.

Table 6. Vertical accelerations of columns and beams for the fixed base option – HVPS record.

Fixed Base											
Story	*C1*	*B1*	*B2*	*C2*	*B3*	*B4*	*C3*	*B5*	*B6*	*B7*	*C4*
ST 5	*2.1*	*5.6*	*5.9*	*2.6*	*5.3*	*5.1*	*2.4*	*4.8*	*6.6*	*4.3*	*3.2*
ST 4	*2.0*	*4.0*	*4.5*	*2.4*	*4.9*	*4.8*	*2.3*	*5.1*	*7.0*	*5.0*	*3.1*
ST 3	*1.9*	*4.0*	*4.4*	*2.1*	*3.7*	*3.6*	*2.0*	*3.8*	*5.3*	*4.3*	*2.9*
ST 2	*1.9*	*3.2*	*3.5*	*1.7*	*3.2*	*3.0*	*1.9*	*2.9*	*4.3*	*2.9*	*2.5*
ST 1	*1.9*	*2.6*	*2.6*	*1.7*	*2.7*	*2.8*	*1.7*	*3.9*	*5.0*	*3.3*	*2.2*
G.F.	*2.1*			*2.1*			*2.1*				*2.1*

Table 3. Vertical accelerations of columns and beams for the CSI option – HVPS record.

Conventional Seismic Isolation (CSI)											
Story	*C1*	*B1*	*B2*	*C2*	*B3*	*B4*	*C3*	*B5*	*B6*	*B7*	*C4*
ST 5	*4.6*	*4.7*	*5.2*	*4.2*	*4.6*	*5.1*	*4.6*	*6.6*	*9.3*	*7.0*	*4.7*
ST 4	*4.4*	*4.4*	*4.8*	*4.0*	*4.6*	*5.5*	*4.5*	*5.0*	*6.7*	*5.4*	*4.6*
ST 3	*4.0*	*4.3*	*5.0*	*3.8*	*4.6*	*4.9*	*4.2*	*5.0*	*6.7*	*5.3*	*4.3*
ST 2	*3.9*	*4.0*	*4.6*	*3.6*	*4.3*	*4.6*	*3.8*	*4.3*	*5.8*	*4.4*	*4.1*
ST 1	*4.0*	*3.9*	*4.2*	*3.9*	*4.0*	*4.3*	*3.8*	*4.8*	*6.4*	*5.3*	*4.1*
*TI. **	*3.9*			*3.9*			*4.2*				*4.7*
*BI. ***	*2.2*			*2.2*			*2.2*				*2.2*

Table 4. Vertical accelerations of columns and beams for the 3DSI option – HVPS record.

Three Dimensional Seismic Isolation (3DSI)											
Story	*C1*	*B1*	*B2*	*C2*	*B3*	*B4*	*C3*	*B5*	*B6*	*B7*	*C4*
ST 5	*1.6*	*2.2*	*2.1*	*1.7*	*2.3*	*2.3*	*1.8*	*2.5*	*3.3*	*2.9*	*2.2*
ST 4	*1.6*	*2.0*	*2.2*	*1.6*	*2.1*	*2.1*	*1.8*	*1.9*	*2.7*	*1.9*	*2.2*
ST 3	*1.5*	*2.0*	*2.2*	*1.5*	*2.0*	*1.9*	*1.7*	*1.8*	*2.6*	*2.2*	*2.1*
ST 2	*1.5*	*1.9*	*2.0*	*1.5*	*1.9*	*2.0*	*1.7*	*1.7*	*2.4*	*2.1*	*2.1*
ST 1	*1.5*	*1.9*	*1.8*	*1.5*	*1.9*	*2.0*	*1.7*	*1.7*	*2.5*	*2.1*	*2.0*
*TI. **	*1.6*			*1.6*			*1.8*				*2.1*
*BI. ***	*2.2*			*2.2*			*2.2*				*2.2*

*Top of Isolation level.

**Bottom of Isolation level.

To better understand the efficiency of the proposed system, Figure. 7 illustrates the distribution of acceleration along the beams under the HVPS record at level 1 and level 5. This figure implies that: a) The maximum vertical acceleration (VA) at the middle of the long beam has dramatically decreased by up to 65% (from 9.3g to 3.3g) under the HVPS record. On average, it is about 57% (from 4.89 to 2.06), indicating that the efficiency of the proposed 3DSI system increases under higher vertical PGAs. b) On average, the acceleration amplification due to the beam vibrations is more than 250% for F.B. and CSI systems, while it is reduced to about 170% for the 3DSI system. The higher vertical period of the 3DSI system has mitigated the influence of beam vibration, which causes acceleration amplification.

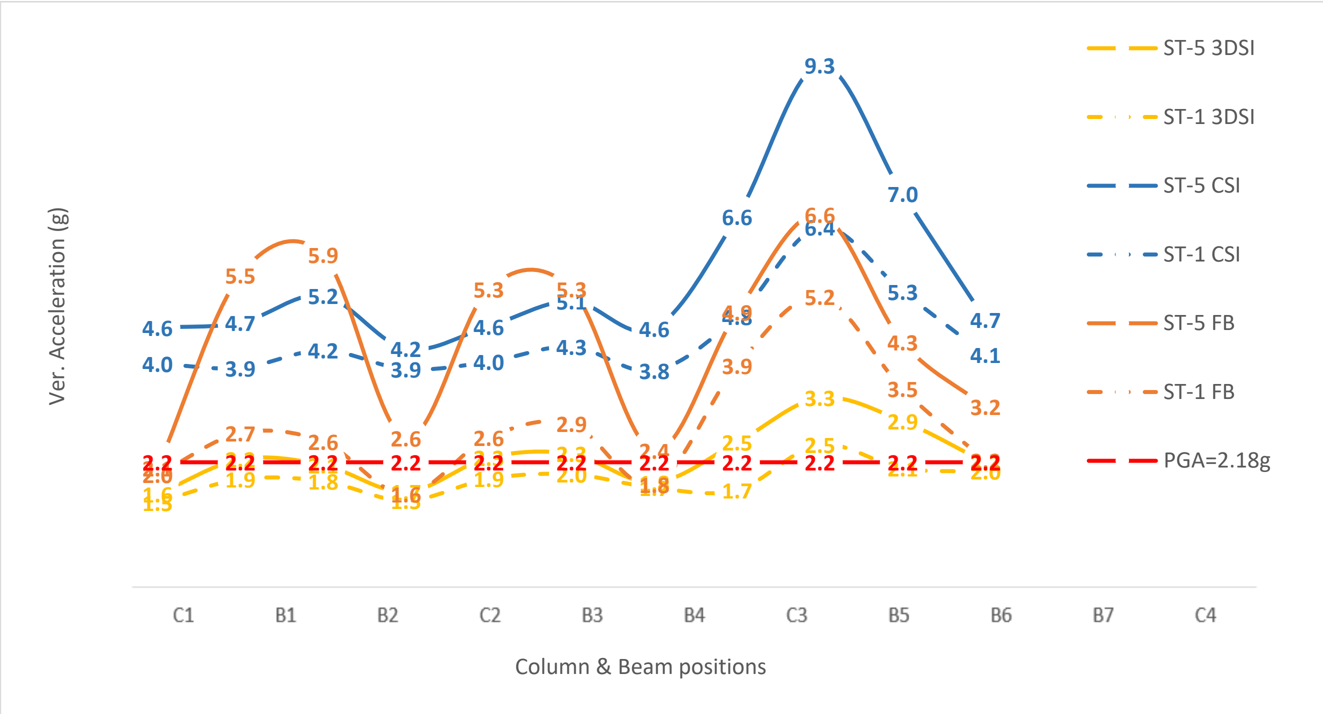

Figure. 4. HVPS vertical acceleration distribution of columns and beams at levels 1&5.

Figure. 8 illustrates the trend of vertical accelerations along the height for the HVPS record at C1 and B6, which was also observed for other records. The figure shows that the 3DSI system causes an almost uniform distribution from the top of the isolation upward. In contrast, the FB option presents a straight distribution on the columns while significantly amplifying across the beams. For the CSI system, the vertical accelerations dramatically increased by up to four times of the vertical PGA on the middle of the long beam.

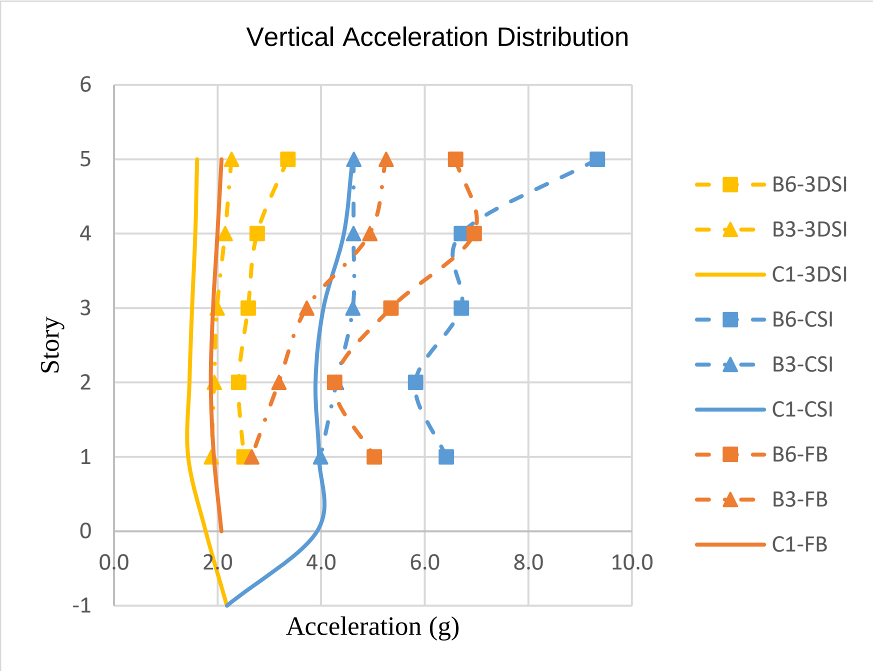

Figure. 5. Vertical acceleration distribution along with the height for C1 & B6 – HVPS record.

6 CONCLUSION

Conventional Seismic Isolation (CSI) systems have demonstrated their efficacy in mitigating seismic responses within the horizontal plane. However, their performance in the vertical direction is comparatively limited. This shortcoming necessitates the implementation of Three Dimensional Seismic Isolation (3DSI) systems, particularly in near-field regions with high vertical Peak Ground Accelerations (PGA).

This research study assesses the effectiveness of a proposed 3DSI system in diminishing structural responses in a five-story building compared with the Fixed Base (F.B.) and CSI alternatives. The following conclusions emerge from this investigation:

•The proposed 3DSI system attenuated vertical accelerations by up to 65% compared to the CSI system, resulting in lower levels of non-structural damage. Additionally, the trend of vertical accelerations along the height showed an escalation trend for F.B. and CSI systems, while the 3DSI system led to a more uniform distribution along the height.

•CSI and 3DSI systems significantly reduced the lateral forces on columns compared to fixed-base buildings, but the CSI option caused compression/tension forces to vary about ±10.0% from the F.B. system. The 3DSI system offered 20% less lateral forces than the CSI system and approximately 50% and 25% less compression and tension axial loads, respectively.

•The proposed 3DSI system is tuneable in both horizontal and vertical directions according to the project's specifications. This study targeted a vertical period of Tv=0.3s, which effectively mitigated horizontal-vertical responses. A higher vertical period is achievable by adjusting the specifications and numbers of SHDR layers.

Overall, this research demonstrates that the proposed 3DSI system is highly effective in reducing the seismic responses of buildings compared to F.B. and CSI options. It offers more level of safety for the building's occupants and equipment, making it an attractive option for seismic isolation in near-field zones with high vertical PGA.

7 ACKNOWLEDGEMENTS

Special thanks to those have assisted to this research, in particular the technical support from Low Damage Design Co.

8 REFERENCES

ASCE 7-22. 2022. *Minimum Design Loads and Associated Criteria for Buildings and Other Structures.* LCCN 20170182751. American Society of Civil Engineers.

BS EN 15129. 2018. *European Standard on Anti-Seismic Devices*. BSI Standard Publication.

Cancellara, Donato, and Fabio De Angelis. 2016. "Nonlinear Dynamic Analysis for Multi-Storey RC Structures with Hybrid Base Isolation Systems in Presence of Bi-Directional Ground Motions." *Composite Structures* 154 (October): 464–92. https://doi.org/10.1016/j.compstruct.2016.07.030.

Cimellaro, Gian Paolo, Marco Domaneschi, and Gordon Warn. 2018. "Three-Dimensional Base Isolation Using Vertical Negative Stiffness Devices." *Journal of Earthquake Engineering*, August, 1–29. https://doi.org/10.1080/13632469.2018.1493004.

Constantinou, M.C., A.S. Whittaker, Y. Kalpakidis, D.M. Fenz, and G.P. Warn. 2007. *Performance of Seismic Isolation Hardware under Service and Seismic Loading: MCEER-07-0012*.

Dong, Wenqing, Yundong Shi, Qi Wang, Yuchen Wang, and Jia-Bao Yan. 2023. "Development of a Long-Period Vertical Base Isolation Device with Variable Stiffness for Steel Frame Structures." *Soil Dynamics and Earthquake Engineering* 164 (January): 107638. https://doi.org/10.1016/j.soildyn.2022.107638.

Eltahawy, Walaa, Keri L. Ryan, Sevki Cesmeci, and Faramarz Gordaninejad. 2018. "Parameters Affecting Dynamics of Three-Dimensional Seismic Isolation." *Journal of Earthquake Engineering* 0 (0): 1–26. https://doi.org/10.1080/13632469.2018.1537902.

FEMA. 2003. *Multi-Hazard Loss Estimation Methodology - Earthquake Model. HAZUS-MH MR4 Technical Manual, Federal Emergency Management Agency, WashIngton.*

FEMA E-74. 2012. "FEMA E-74, Reducing the Risks of Nonstructural Earthquake Damage | FEMA.Gov." 2012. https://www.fema.gov/emergency-managers/risk-management/earthquake/training/fema-e-74.

Fujita, T., S. Fujita, Y. Watanabe, A. Kato, S. Suzuki, and K. Fukumori. 1996. "Fundamental Study of Three-Dimensional Seismic Isolation System for Nuclear Power Plants." In *Proceedings, 11th World Conference on Earthquake Engineering, Acapulco, Mexico*.

Furukawa, Sachi, Eiji Sato, Yundong Shi, Tracy Becker, and Masayoshi Nakashima. 2013. "Full-Scale Shaking Table Test of a Base-Isolated Medical Facility Subjected to Vertical Motions." *Earthquake Engineering & Structural Dynamics* 42 (13): 1931–49. https://doi.org/10.1002/eqe.2305.

Guzman Pujols, Jean C., and Keri L. Ryan. 2018. "Computational Simulation of Slab Vibration and Horizontal-Vertical Coupling in a Full-Scale Test Bed Subjected to 3D Shaking at E-Defense." *Earthquake Engineering & Structural Dynamics* 47 (2): 438–59. https://doi.org/10.1002/eqe.2973.

Inoue, Kazuhiko, Minoru Fushimi, Satoshi Moro, Masaki Morishita, Seiji Kitamura, and Takafumi Fujita. 2004. "Development of Three-Dimensional Seismic Isolation System for next Generation Nuclear Power Plant." In *Proceedings of the 13th World Conference on Earthquake Engineering, Vancouver, BC, Canada*, 1–6.

Koo, Gyeong-Hoi, Jung Jin-Young, Jong-Keun Hwang, Tae-Myung Shin, Lee Min-Seok, and this link will open in a new window Link to external site. 2022. "Vertical Seismic Isolation Device for Three-

Dimensional Seismic Isolation of Nuclear Power Plant Equipment—Case Study.” *Applied Sciences* 12 (1): 320. https://doi.org/10.3390/app12010320.

Mazza, Fabio, and Rodolfo Labernarda. 2017. “Structural and Non-Structural Intensity Measures for the Assessment of Base-Isolated Structures Subjected to Pulse-like near-Fault Earthquakes.” *Soil Dynamics and Earthquake Engineering* 96 (May): 115–27. https://doi.org/10.1016/j.soildyn.2017.02.013.

Morishita, Masaki, Kazuhiko Inoue, and Takafumi Fujita. 2004. “Development of Three-Dimensional Seismic Isolation Systems for Fast Reactor Application.” *Journal of Japan Association for Earthquake Engineering* 4 (3): 305–10.

Pourmasoud, Mohammad Masoud, James B. P. Lim, Iman Hajirasouliha, and Daniel McCrum. 2020. “Multi-Directional Base Isolation System for Coupled Horizontal and Vertical Seismic Excitations.” *Journal of Earthquake Engineering*, January, 1–26. https://doi.org/10.1080/13632469.2020.1713925.

Ryan, Keri L., Siavash Soroushian, E. “Manos” Maragakis, Eiji Sato, Tomohiro Sasaki, and Taichiro Okazaki. 2016. “Seismic Simulation of an Integrated Ceiling-Partition Wall-Piping System at E-Defense. I: Three-Dimensional Structural Response and Base Isolation.” *Journal of Structural Engineering* 142 (2): 04015130. https://doi.org/10.1061/(ASCE)ST.1943-541X.0001384.

Sarlis, A. A., D. T. R. Pasala, M. C. Constantinou, A. M. Reinhorn, S. Nagarajaiah, and D. P. Taylor. 2013. “Negative Stiffness Device for Seismic Protection of Structures.” *Journal of Structural Engineering* 139 (7): 1124–33. https://doi.org/10.1061/(ASCE)ST.1943-541X.0000616.